JACS
JOURNAL OF THE AMERICAN CHEMICAL SOCIETY
pubs.acs.org/JACS
Article

Rectification in Molecular Tunneling Junctions Based on Alkanethiolates with Bipyridine–Metal Complexes

Junwoo Park, Lee Belding, Li Yuan, Maral P. S. Mousavi, Samuel E. Root, Hyo Jae Yoon, and George M. Whitesides*

Cite This: J. Am. Chem. Soc. 2021, 143, 2156–2163
Read Online
ACCESS | Metrics & More | Article Recommendations | Supporting Information

ABSTRACT: This paper addresses the mechanism for rectification in molecular tunneling junctions based on alkanethiolates terminated by a bipyridine group complexed with a metal ion, that is, having the structure Au^{TS}-S$(CH_2)_{11}$BIPY-MCl_2 (where M = Co or Cu) with a eutectic indium–gallium alloy top contact (EGaIn, 75.5% Ga 24.5% In). Here, Au^{TS}-S$(CH_2)_{11}$BIPY is a self-assembled monolayer (SAM) of an alkanethiolate with 4-methyl-2,2′-bipyridine (BIPY) head groups, on template-stripped gold (Au^{TS}). When the SAM is exposed to cobalt(II) chloride, SAMs of the form Au^{TS}-S$(CH_2)_{11}$BIPY-$CoCl_2$ rectify current with a rectification ratio of $r^+ = 82.0$ at ±1.0 V. The rectification, however, disappears ($r^+ = 1.0$) when the SAM is exposed to copper(II) chloride instead of cobalt. We draw the following conclusions from our experimental results: (i) Au^{TS}-S$(CH_2)_{11}$BIPY-$CoCl_2$ junctions rectify current because only at positive bias (+1.0 V) is there an accessible molecular orbital (the LUMO) on the BIPY-$CoCl_2$ moiety, while at negative bias (−1.0 V), neither the energy level of the HOMO or the LUMO lies between the Fermi levels of the electrodes. (ii) Au^{TS}-S$(CH_2)_{11}$BIPY-$CuCl_2$ junctions do not rectify current because there is an accessible molecular orbital on the BIPY-$CuCl_2$ moiety at both negative and positive bias (the HOMO is accessible at negative bias, and the LUMO is accessible at positive bias). The difference in accessibility of the HOMO levels at −1.0 V causes charge transfer—at negative bias—to take place via Fowler–Nordheim tunneling in BIPY-$CoCl_2$ junctions, and via direct tunneling in BIPY-$CuCl_2$ junctions. This difference in tunneling mechanism at negative bias is the origin of the difference in rectification ratio between BIPY-$CoCl_2$ and BIPY-$CuCl_2$ junctions.

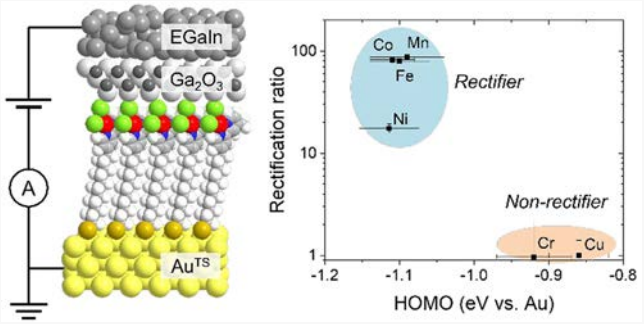

INTRODUCTION

When charge passes through a molecule connected by two electrodes, if the rate of charge transport (CT) in one direction is different than in the opposite direction (at the same magnitude of applied voltage), the molecular junction *rectifies* current, and is relevant to the subject of molecular rectifiers.[1−12] Rectification is especially useful in mechanistic studies of charge transport through molecular junctions because the same junction is used to measure tunneling currents at both positive and negative bias voltage. The commonality reduces errors due to junction-to-junction variability in the measurement of current.[13−21]

We previously reported that molecular junctions composed of BIPY-terminated *n*-alkanethiol-based self-assembled monolayers (SAMs) on template-stripped metal surfaces rectify current.[22,23] We have observed that the conductive properties (including rectification) of these BIPY junctions can change drastically upon exposure to metal ions. This paper describes the rectification of tunneling currents at ±1.0 V in junctions with the structure Au^{TS}-S$(CH_2)_{11}$BIPY-M//GaO_x/EGaIn, where M = Co or Cu (Figure 1). The objective of this paper is to understand why tunneling currents differ between BIPY-$CoCl_2$ junctions and BIPY-$CuCl_2$ junctions.

SAMs based on metal complexes of BIPY are an excellent model system to investigate molecular rectifiers classified as having an asymmetrically positioned chromophore in their molecular structure (e.g., molecules composed of an insulating alkyl chain terminated by a more conducting, aromatic moiety) for two reasons. First, the ability for BIPY to form complexes with transition metal ions makes it possible to modify the frontier energy levels of the BIPY-MCl_2 group. A survey of the effects of different metal ions (Cr, Mn, Fe, Co, Ni, or Cu) showed that BIPY-$CoCl_2$ and BIPY-$CuCl_2$ junctions exhibited pronounced differences in rectification. The differences in rectification between BIPY-$CoCl_2$ and BIPY-$CuCl_2$ junctions

Received: December 4, 2020
Published: January 22, 2021

Downloaded via HARVARD UNIV on February 23, 2021 at 13:58:17 (UTC).
See https://pubs.acs.org/sharingguidelines for options on how to legitimately share published articles.

ACS Publications
© 2021 American Chemical Society

https://dx.doi.org/10.1021/jacs.0c12641
J. Am. Chem. Soc. 2021, 143, 2156–2163

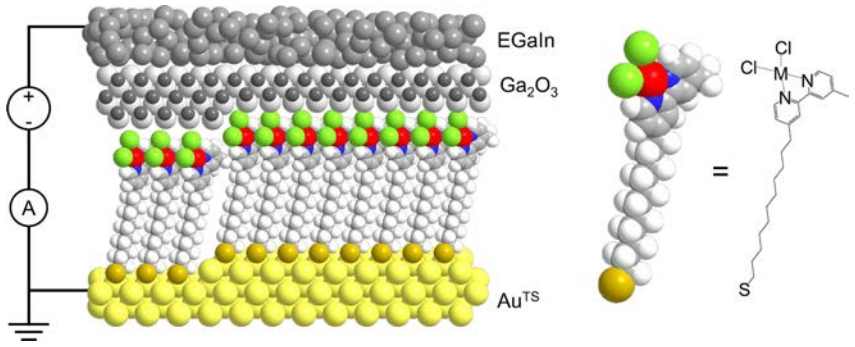

Figure 1. Schematic images of the molecular junction with the structures of Au^{TS}-$S(CH_2)_{11}$BIPY-MCl_2//GaO_x/EGaIn. XPS results show a 1:1 ratio between the metal and the 2,2′-bipyridine group. In reality, interfaces at EGaIn are rough, and the Au surface is not perfectly flat. Detailed descriptions of molecular structure are summarized in the Supporting Information.

Table 1. Elemental Ratios in the Au^{TS}-$S(CH_2)_{11}$BIPY-$CoCl_2$ and Au^{TS}-$S(CH_2)_{11}$BIPY-$CuCl_2$ Junctions Characterized by XPS[a]

Junctions	Sulfur:Nitrogen	Sulfur:Nitrogen (corrected for thickness of SAMs)	Metal:Nitrogen	Metal:Chloride
BIPY-$CoCl_2$	1:2.7 ± 0.05	1:1.8 ± 0.04	1:1.8 ± 0.14	1:1.8 ± 0.06
BIPY-$CuCl_2$	1:2.7 ± 0.08	1:1.8 ± 0.05	1:1.9 ± 0.12	1:1.7 ± 0.16

[a]Raw data is in the Supporting Information. Experiments were replicated a total of nine times, and uncertainty values represent the standard deviation.

suggests that rectification is determined purely by the electronic structure of the molecular junction, as opposed to (a) asymmetry in the nature of the two electrodes (Au bottom-electrode and EGaIn top-electrode), (b) asymmetry in the top and bottom contacts (covalent Au−S bond at bottom-electrode and a van der Waals contact with the EGaIn), (c) redox reactions involving EGaIn, or (d) the oxide layer of EGaIn. Second, BIPY-MCl_2 junctions, in principle, have the same supramolecular structure, which eliminates the uncertainty associated with differences in packing density, orientation, and conformation.

RESULTS AND DISCUSSION

BIPY-$CoCl_2$ and BIPY-$CuCl_2$ SAMs both have 1:1 (M:BIPY) binding ratios. X-ray photoelectron spectroscopy (XPS) was employed to characterize the elemental composition of the BIPY-MCl_2 SAMs, using a total of nine samples. The atomic ratio of nitrogen to sulfur in the SAMs was determined to 1.8 ± 0.04 for BIPY-$CoCl_2$ SAMs and 1.8 ± 0.05 for BIPY-$CuCl_2$ SAMs, after correcting for attenuation of the sulfur signal due to the SAM thickness (Table 1; see Supporting Information for details). These values agree with the ratio measured for BIPY SAMs (1.79 ± 0.04),[24] demonstrating BIPY-$CoCl_2$ and BIPY-$CuCl_2$ SAMs have a similar ratio of nitrogen to sulfur relative to one another, and to uncomplexed BIPY SAMs. These observations indicate that the core structure of the SAMs remain unchanged upon metal complexation. The ratios of nitrogen to metal were 1.8 ± 0.14 for BIPY-$CoCl_2$ junctions and 1.9 ± 0.12 for BIPY-$CuCl_2$ junctions. The ratios strongly suggested that metal and the surface-bound 2,2′-bipyridine form a 1:1 BIPY·M^{2+} complex. Figure 1 shows the schematic images of the molecular junction (details about possible arrangements are described in the Supporting Information).[25,26] The ratio of chloride to metal in these junctions was measured to be 1.8 ± 0.06 for BIPY-$CoCl_2$ junctions and 1.7 ± 0.16 for BIPY-$CuCl_2$ junctions. The substoichiometric Cl^- ion signal may be the result of an exchange between Cl^- and hydroxide upon contact of the SAM surface with trace water in the atmosphere, or in the ethanolic solution during the preparation of the SAM. The species of anion could affect the change of energy levels in molecular junctions. The averaged $J(V)$ traces measured in BIPY-$CoCl_2$ and BIPY-$CuCl_2$ junctions which complexed with other halide anions, however, still showed no significant change in rectification (Figure S4).

BIPY-$CoCl_2$ junctions rectify current while BIPY-$CuCl_2$ junctions do not. Figures 2a and b show averaged $J(V)$ curves recorded on BIPY-$CoCl_2$ (548 traces on 26 junctions) and BIPY-$CuCl_2$ junctions (357 traces on 17 junctions) using the EGaIn measurement system. We report the rectification ratio, r^+, as the ratio of current density at a given positive and negative bias ($r^+ = |J(+V)|/|J(-V)|$ at ±1 V). As shown in Figure 2c, BIPY-$CoCl_2$ junctions rectified tunneling current with a rectification ratio (r^+) of 82.0. In BIPY-$CuCl_2$ junctions, however, we did not observe rectification (r^+ = 1.0 at ±1.0 V).

The difference in rectification between BIPY-$CoCl_2$ and BIPY-$CuCl_2$ junctions is the result of a difference in their mechanisms of tunneling at negative bias. The largest difference in the magnitude of J(V) occurs at negative bias, where BIPY-$CuCl_2$ junctions have a 33× larger tunneling current than BIPY-$CoCl_2$ junctions. At positive bias, the difference in the rate of charge tunneling between BIPY-$CoCl_2$ and BIPY-$CuCl_2$ is much smaller (the rate of tunneling is only ~2× larger in BIPY-$CoCl_2$ junctions).[22] This observation—that complexation with copper increases the rate of tunneling at negative bias—led us to hypothesize that an additional conduction path (the HOMO) may be accessible at negative bias in BIPY-$CuCl_2$, but not in BIPY-$CoCl_2$ junctions. To assess this hypothesis, we measured the approximate HOMO energy levels of both the BIPY-$CoCl_2$ and BIPY-$CuCl_2$ junctions, using both cyclic voltammetry (CV) and ultraviolet photoelectron spectroscopy (UPS).

The HOMO of BIPY-$CuCl_2$, but not BIPY-$CoCl_2$, lies between the Fermi level of the two electrodes at −1.0 V. We first characterized the $S(CH_2)_{11}$BIPY-$CoCl_2$ and $S(CH_2)_{11}$BIPY-$CuCl_2$ SAMs on a Au^{TS} surface with CV (Figure 3) in 0.1 M aqueous $KClO_4$ electrolyte solutions, using a Pt counter electrode, and an Ag/AgCl reference electrode. The scan rate was 0.1 V/s. For BIPY-$CoCl_2$ SAMs, no redox peak was

https://dx.doi.org/10.1021/jacs.0c12641
J. Am. Chem. Soc. 2021, 143, 2156−2163

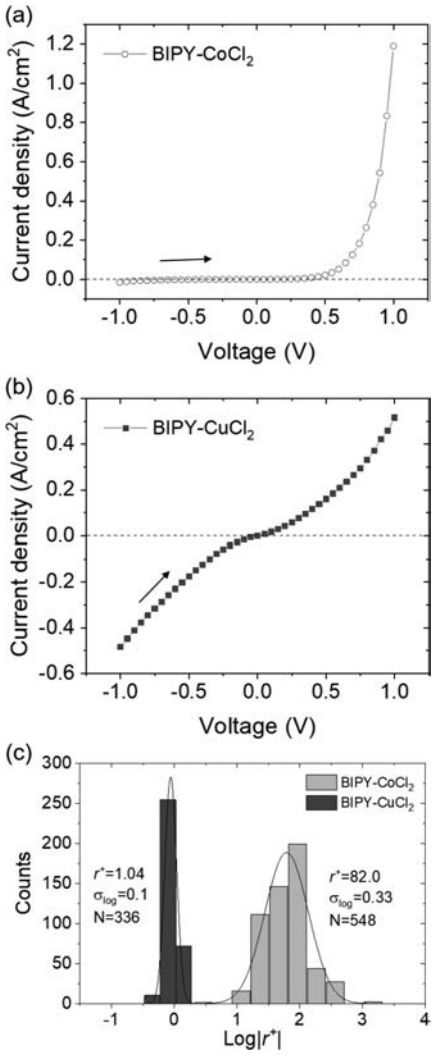

Figure 2. Averaged $J(V)$ traces of (a) BIPY-$CoCl_2$ and (b) BIPY-$CuCl_2$ junctions. (c) Histograms of log|r^+| of the BIPY-$CoCl_2$ and BIPY-$CuCl_2$ junctions at ±1.0 V with a Gaussian fit to the histograms.

observed within the potential range of −0.2−1.0 V (vs Ag/AgCl in 1.0 M KCl (aq)). Outside of this potential window, new peaks appeared in the CV, which increased in peak height after each scan—and are thus assumed to be caused by damage to SAM (Figure S5). For this reason, we limited the voltage applied to the working electrode to −0.2 to +1.0 V. The BIPY-$CuCl_2$ SAMs, on the other hand, showed well-defined, reversible anodic (E_{pa} = ∼470 mV) and cathodic (E_{pc} = ∼350 mV) peaks within the −0.2 to +1.0 V window (Figure 3). We assume that these peaks are indicative of oxidation/reduction reactions between BIPY-$Cu^{2+}Cl_2$ + e^- ↔ BIPY-Cu^+Cl.[27] We observed a peak separation of approximately ∼120 mV between the anodic and cathodic peaks. For an ideal, reversible redox reaction, the peak separation should be zero. Previous CV measurements on similar systems, however, are also characterized by finite values of peak separation.[28,29] The redox process in the CV of the BIPY-$CuCl_2$ SAM is only partially reversible. We believe that a plausible origin of the irreversibility of the process is the dissociation of Cu^{2+} cations from the SAMs at rates comparable with the time scale of the CV experiments.

The energy level of the HOMO (E_{HOMO}) relative to vacuum can be estimated from the formal half-wave potential $E_{1/2}$ obtained from the cyclic voltammogram (eq 1).[30]

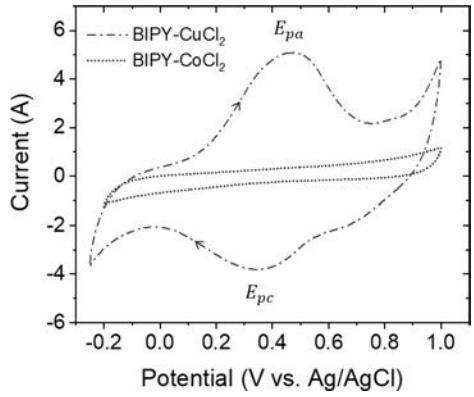

Figure 3. Cyclic voltammograms of SAMs of $S(CH_2)_{11}$BIPY-$CoCl_2$ and $S(CH_2)_{11}$BIPY-$CuCl_2$ on template-stripped Au. The measurements were run in aqueous 0.1 M $KClO_4$ solutions, using a Ag/AgCl reference electrode immersed in 1.0 M KCl (aq), and a Pt counter electrode. The SAMs were formed by immersion of a Au^{TS} surface (∼1 cm^2) in 1.0 mM ethanolic solutions of thiol-terminated molecules for 18 h under a nitrogen atmosphere. Metal ions were combined with the BIPY-terminated SAMs using an ethanolic solution of 10 mM metal(II) chloride under a nitrogen atmosphere for 18 h. The BIPY-$CuCl_2$ SAMs showed reversible anodic (E_{pa} = ∼470 mV) and cathodic (E_{pc} = ∼350 mV) peaks. The CV of the SAM of $S(CH_2)_{11}$BIPY is in Figure S6.

$$E_{HOMO} = E_{abs,NHE} - eE_{1/2,NHE} \quad (1)$$

where $E_{abs,NHE}$ is the absolute potential energy (−4.5 eV) of the normal hydrogen electrode (NHE), and $E_{1/2,NHE}$ is the $E_{1/2}$ vs the NHE. The $E_{1/2,NHE}$ of the $S(CH_2)_{11}$BIPY-$CuCl_2$ ($E_{1/2,NHE,BIPY\text{-}Cu}$) was 0.60 V, which gave a value for $E_{HOMO,BIPY\text{-}Cu}$ of −5.10 eV. This value of E_{HOMO} for BIPY-$CuCl_2$ is −0.80 eV with respect to the Fermi level of Au and is thus accessible when −1.0 V is applied to the junction.

We also characterized the HOMO levels of Au^{TS}-$S(CH_2)_{11}$BIPY-$CoCl_2$ and Au^{TS}-$S(CH_2)_{11}$BIPY-$CuCl_2$ SAMs using UPS (Figure S6). Based on the UPS results, the HOMO level of BIPY-$CoCl_2$ was −1.11 eV, and that of BIPY-$CuCl_2$ was −0.86 eV, with respect to the Fermi level of Au^{TS}. The energy level of the HOMO for BIPY-$CuCl_2$ determined by UPS (−0.86 eV) was almost equal to the value obtained from CV (−0.80 eV). This result indicates that the HOMO level of the BIPY-$CuCl_2$ moiety *is involved* (accessible) in the tunneling process at −1.0 V. Because the HOMO level of BIPY-$CoCl_2$, however, is more than 1.0 eV below the Fermi level of the Au electrode, it is *not involved* (inaccessible) at −1.0 V. These results are consistent with our original hypothesis, that the accessibility of molecular orbitals at negative bias is directly correlated with the magnitude of current density at that bias and the overall rectification ratio.

Temperature Dependence of Tunneling Rates. Tunneling is a temperature-independent process, and evidence of temperature dependence in measurements of charge transport is generally associated with an electron hopping step. Electron hopping involves a formal redox process—however fleeting—and thus requires an energetically accessible molecular orbital. Thus, variable temperature measurements can be used to differentiate between a pure tunneling mechanism of charge transport and a mechanism that involves hopping. In these experiments, the EGaIn tip was gently brought into contact with the samples and the Au^{TS}-$S(CH_2)_{11}$BIPY-MCl_2//GaO_x/EGaIn junction was encapsulated by a photocurable polymer (Norland Optical Adhesive 61, Norland Products). Then, we gently lifted the syringe containing EGaIn to form encapsulated BIPY-MCl_2

https://dx.doi.org/10.1021/jacs.0c12641
J. Am. Chem. Soc. 2021, 143, 2156−2163

junctions to allow for transfer to an environmentally controlled probe station (Lakeshore 1.5K Probe Station).[31]

Figure 4 shows the results of variable temperature measurements of charge transport across the BIPY-$CoCl_2$ and BIPY-$CuCl_2$ junctions at −1.0 V and +1.0 V. At +1.0 V, the values of current density in both BIPY-$CuCl_2$ and BIPY-$CoCl_2$ junctions change with temperature. This temperature dependence implies that there is an accessible molecular orbital at +1.0 V (see Supporting Information for details). At −1.0 V, however, the current density in BIPY-$CoCl_2$ junctions does not change with temperature, while in BIPY-$CuCl_2$ junctions, it does. This result supports our previous CV and UPS data on the relative position of the HOMO levels of BIPY-$CoCl_2$ and BIPY-$CuCl_2$, as well as our mechanistic interpretation that the HOMO of BIPY-$CuCl_2$ is *accessible* at −1.0 V, while the HOMO of BIPY-$CoCl_2$ is *inaccessible*. Interestingly, we observed a similar dependence on temperature for the current densities at both positive and negative biases for BIPY-$CuCl_2$. This symmetry suggests a similar activation energy for the hopping step at either bias. We do not believe that this symmetry must necessarily exist for all junctions of this type. Moreover, in comparison to the uncomplexed BIPY junction,[23] we observed that the BIPY-$CoCl_2$ junction exhibited a difference in the dependence of current density on temperature (Figure S8).

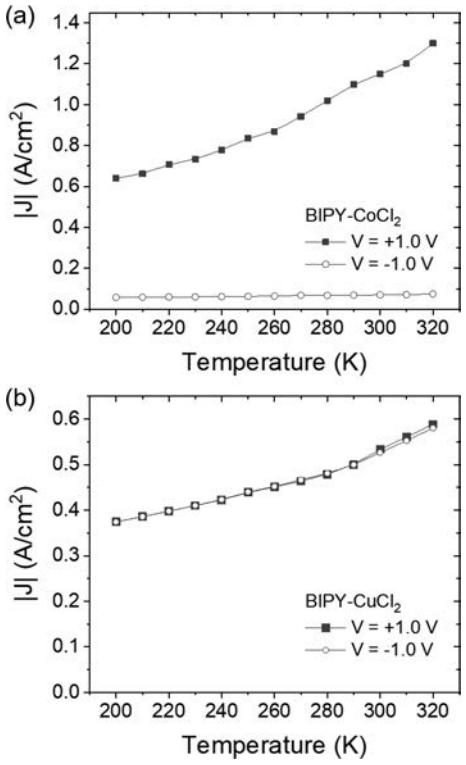

Figure 4. Values of current density measured at −1.0 V and +1.0 V as a function of temperature in (a) BIPY-$CoCl_2$ junctions and (b) BIPY-$CuCl_2$ junctions. The variable temperature experiments were performed with a probe station (Lakeshore 1.5K Probe Station) in vacuum (1×10^{-9} bar).

Mechanism for Differences in Tunneling Currents between BIPY-MCl_2 Complexes. Figure 5a and 5b are schematic representations of the energy level diagrams of the BIPY-$CoCl_2$ and BIPY-$CuCl_2$ junctions at −1.0 V and +1.0 V, based on the results of our experiments. The HOMO and LUMO are centered on the BIPY-MCl_2 complex, and are thus isolated from the alkyl chain (i.e., the rectangles representing these MOs do not span the entire width of the barrier) and are in close contact with the GaO_x/EGaIn electrode. As a result of their proximity to the GaO_x/EGaIn electrode, the HOMO and LUMO of the junction are coupled to the energy level of the GaO_x/EGaIn electrode, a phenomenon known as Fermi level pinning.[15]

Our mechanistic proposal suggests that the *inaccessible* HOMO of BIPY-$CoCl_2$ at −1.0 V and the *accessible* LUMO at +1.0 V is the origin of the rectification in BIPY-$CoCl_2$ junctions. We believe that a MO that is energetically accessible, and is localized at one end of the molecule, reduces the width of the barrier by approximately the size of the MO (which in this system, is located on the BIPY-MCl_2 complex). This reduction in barrier width is concomitant with an increased rate of charge transport.

The Fowler−Nordheim (FN) plots in Figure 6 distinguish between direct tunneling and FN tunneling across the BIPY-MCl_2 junctions and support our mechanistic interpretation of charge transport in these systems. BIPY-$CoCl_2$ and BIPY-$CuCl_2$ show distinctly different graphical features in the FN plots. Most notably, while BIPY-$CuCl_2$ junctions show predominantly direct tunneling throughout the entire negative bias window, BIPY-$CoCl_2$ junctions have a transition in the conduction mechanism from direct tunneling to FN tunneling at both negative and positive bias. That is, above a threshold voltage (known as the transition voltage),[32] they show a clear linear dependence of $\ln(J/V^2)$ on $1/V$.

For BIPY-$CoCl_2$ junctions, at −1.0 V, the HOMO level (−4.41 eV) is lower in energy than the Fermi level of the Au electrode (−4.3 eV) and *is* thus *not* involved in the charge transfer process. The FN plot of the BIPY-$CoCl_2$ junctions shows that, at −1.0 V, the conduction mechanism of BIPY-$CoCl_2$ junctions is FN tunneling (Figure 6a). These two results are consistent with the energy level diagram in Figure 5a. At positive bias (+1.0 V), the conduction mechanism for BIPY-$CoCl_2$ is also FN tunneling. This result supports our interpretation of the variable temperature experiments, because conventional understanding of band structure (which admittedly may not be complete or accurate) suggests that, for a system in which the LUMO is localized adjacent to the ungrounded electrode, FN tunneling at +1.0 V is impossible without an accessible MO. That is, FN tunneling at +1.0 V strongly suggests that the LUMO of the BIPY-$CoCl_2$ moiety *is* energetically accessible for charge transfer at +1.0 V (Figure 6b).

For BIPY-$CuCl_2$ junctions, the results of our CV, UPS, and variable temperature experiments all suggest that the HOMO is energetically accessible at −1.0 V. The FN plot in Figure 6b shows only direct tunneling between 0 and −1.0 V, which is consistent with the energy diagram in Figure 5a involving an accessible HOMO. This mechanistic interpretation is also consistent with the higher rate of charge transport in BIPY-$CuCl_2$ junctions than in BIPY-$CoCl_2$ junctions, at −1.0 V. Again, we believe that the accessible HOMO in the BIPY-$CuCl_2$ junction decreases the width of the barrier. At positive bias, the FN plot for the BIPY-$CuCl_2$ junctions (Figure 6b) shows a transition from direct tunneling to FN tunneling close to the +1.0 V region (the transition becomes clear when the applied bias is increased to +1.5 V; see Supporting Information for details). This result is consistent with the energy diagram in Figure 5b, which involves an accessible LUMO at +1.0 V. As is the case at negative bias, due to the accessible LUMO of BIPY-$CuCl_2$ at +1.0 V, the barrier width across the junction is reduced,

https://dx.doi.org/10.1021/jacs.0c12641
J. Am. Chem. Soc. 2021, 143, 2156−2163

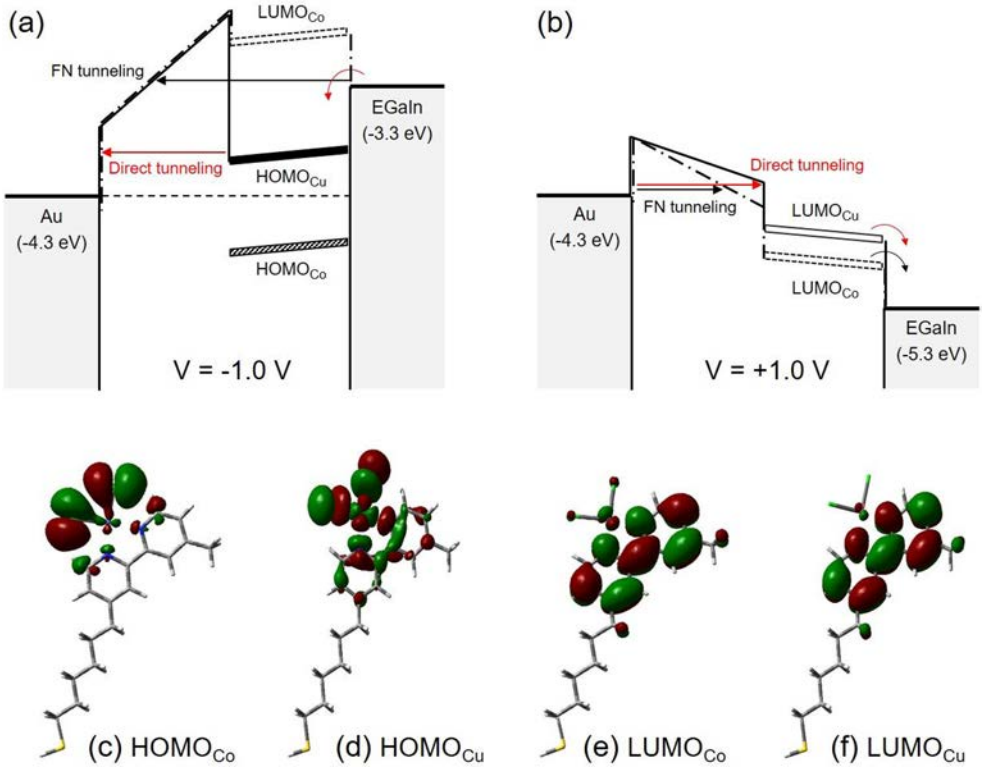

Figure 5. Schematic representations of the proposed energy level diagrams of BIPY-$CoCl_2$ and BIPY-$CuCl_2$ junctions (a) at −1.0 V and (b) at +1.0 V bias. The bottom template-stripped Au electrode is grounded, and we biased the GaO_x/EGaIn top electrode. The black dash-dotted and black solid lines represent the potential barrier (heights and widths) in BIPY-$CoCl_2$ and BIPY-$CuCl_2$ junctions, respectively. We do not know the exact values of LUMOs or the HOMO−LUMO gap. In real molecular junctions, the potential drops near the metal/molecule interfaces are greater than those within the molecule (i.e., the potential barrier is not a straight line). Here, we use a straight line for visual convenience. Also, the black and red arrows indicate the tunneling path of charges across the BIPY-$CoCl_2$ and BIPY-$CuCl_2$ junctions, respectively. The black dashed line in (a) was added to emphasize the position of the Fermi level of Au with respect to the HOMOs of conducting moieties. Geometry of molecular orbitals calculated by density functional theory (DFT): HOMO of (c) BIPY-$CoCl_2$ and (d) BIPY-$CuCl_2$ and LUMO of (e) BIPY-$CoCl_2$ and (f) BIPY-$CuCl_2$.

and the rate of charge transport is nearly the same as that at −1.0 V. Thus, we suppose that the *accessible* HOMO at −1.0 V and the *accessible* LUMO at +1.0 V are why no rectification is observed in BIPY-$CuCl_2$ junctions.[30]

These results, taken together, suggest that, at −1.0 V, the increased rate of tunneling (×33) of SAMs of BIPY-$CuCl_2$ compared to BIPY-$CoCl_2$ is the result of the presence of an accessible HOMO in the BIPY-$CuCl_2$ junction (Figure 5a and 5b); the corresponding orbital is not accessible in the BIPY-$CoCl_2$ junction. For BIPY-$CuCl_2$ junctions, the mechanism consists of a hopping step to the BIPY-$CuCl_2$ unit and then a direct tunneling step across the alkyl chain. By contrast, for BIPY-$CoCl_2$ junctions, due to the inaccessibility of the HOMO level, the mechanism consists of FN tunneling across the entire molecule. At +1.0 V, the decreased rate of tunneling (×2) of SAMs of BIPY-$CuCl_2$ compared to BIPY-$CoCl_2$ arises principally from differences in the barrier height at the alkyl/BIPY-MCl_2 interfaces. The mechanism of tunneling in the BIPY-$CoCl_2$ junction consists of FN tunneling across the alkyl chain (therefore we infer a smaller width of the tunneling barrier), followed by a hopping step to the EGaIn electrode. The mechanism of tunneling in the BIPY-$CuCl_2$ junction consists of direct tunneling across the alkyl chain followed by a hopping step to the EGaIn electrode.

Other BIPY-M complexes fit the trend. To support our hypothesis (i.e., the relative position of the HOMOs in BIPY-MCl_2 junctions with respect to the Fermi level of Au electrode determines the occurrence of rectification and the mechanism of tunneling in BIPY-MCl_2 junctions), using the EGaIn junction, we characterized the rectification ratio in BIPY-MCl_2 junctions with other first row transition metals (M = Cr, Mn, Fe, Ni). According to our proposed mechanism, SAMs with a HOMO lower in energy than the Fermi level of Au electrode should rectify current because only at +1.0 V is there an accessible molecular orbital (the LUMO) on the BIPY-MCl_2 moiety and the width of the tunneling barrier at +1.0 V is smaller than that at −1.0 V. Those with HOMOs higher in energy than the Fermi level of Au should not rectify current because there is an accessible molecular orbital on the BIPY-MCl_2 moiety at both negative and positive bias and the widths of tunneling barriers at ±1.0 V are almost identical. In agreement with our proposed mechanism, the SAMs with HOMO energy levels higher than the Au surface—BIPY-$MnCl_2$ (−1.14 eV), BIPY-$FeCl_2$ (−1.10 eV), BIPY-$CoCl_2$ (−1.11 eV), and BIPY-$NiCl_2$ (−1.11 eV) junctions—rectified current (Figure 7), while the SAMs with HOMO energies that are lower than the Au surface—BIPY-$CrCl_2$ (−0.96 eV) and BIPY-$CuCl_2$ (−0.86 eV) junctions—did not rectify current (Figure 7).

Moreover, the junctions that rectified current displayed FN tunneling at −1.0 V (see Supporting Information, Figure S13), while the junctions that did not rectify current, displayed direct tunneling (Figure S13). These results show remarkable consistency with our analysis of the BIPY-$CoCl_2$ and BIPY-$CuCl_2$ junctions. The Supporting Information contains details.

https://dx.doi.org/10.1021/jacs.0c12641
J. Am. Chem. Soc. 2021, 143, 2156−2163

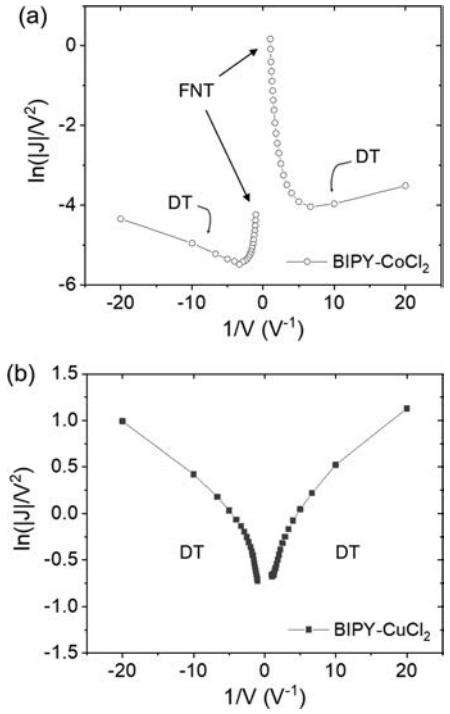

Figure 6. (a) Fowler–Nordheim (FN) plots for BIPY-$CoCl_2$, derived from the current-density data in Figure 2a. A transition in conduction mechanism is observed, beginning with direct tunneling (DT) at lower voltages (logarithmic growth) to FN tunneling (FNT) at higher voltages (linear decay). (b) Fowler–Nordheim (FN) plots for BIPY-$CuCl_2$, derived from the current-density data in Figure 2b.

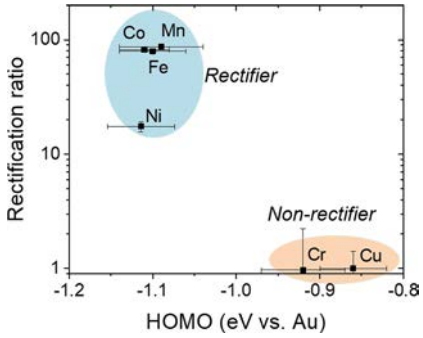

Figure 7. Rectification ratio versus energy of HOMO levels (measured by UPS) of BIPY-MCl_2 junctions.

CONCLUSIONS

In summary, this work describes the mechanism of charge tunneling for $Au^{TS}/S(CH_2)_{11}$BIPY-MCl_2//GaO_x/EGaIn junctions, where M = Co or Cu. The complexation of metal with 2,2′-bipyridine-terminated SAMs changed the nature of rectification (e.g., rectifier or nonrectifier), and the mechanism of tunneling (FN tunneling or direct tunneling) at ±1.0 V. BIPY-$CoCl_2$ junctions rectify current (r^+ = 82.0) at ±1.0 V, while BIPY-$CuCl_2$ junctions do not (r^+ = 1.0). We assert that the rectification observed in BIPY-$CoCl_2$ junctions originates from the electronic structure of the molecules.

Based on CV, UPS measurements, DFT calculations, electrical characterization, and variable temperature experiments, this study reaches four main conclusions:

(i) BIPY-$CoCl_2$ junctions rectify current because only at a positive bias (+1.0 V) is there an accessible molecular orbital (the LUMO) on the BIPY-$CoCl_2$ moiety, while at negative bias (−1.0 V) neither the energy level of the HOMO nor that of the LUMO lie between the Fermi levels of the electrodes.

(ii) BIPY-$CuCl_2$ junctions do not rectify current because there is an accessible molecular orbital on the BIPY-$CuCl_2$ moiety at both negative and positive bias (the HOMO is accessible at negative bias, and the LUMO is accessible at positive bias).

(iii) The difference in accessibility of the HOMO at −1.0 V causes charge transfer—at negative bias—to take place via Fowler–Nordheim tunneling in BIPY-$CoCl_2$ junctions, and via direct tunneling in BIPY-$CuCl_2$ junctions. This difference in tunneling mechanism at negative bias is the origin of the difference in rectification ratio between BIPY-$CoCl_2$ and BIPY-$CuCl_2$ junctions.

(iv) The mechanistic interpretation is also supported by expanding the types of metals in these BIPY-MCl_2 junctions, where M = Cr, Mn, Fe, and Ni. BIPY-M junctions with a low-lying HOMO with respect to the Fermi level of Au (M = Cr and Cu) rectified current, and those with high-lying HOMOs (M = Mn, Fe, Co, and Ni) did not rectify current.

Reliable rules or guidelines for relationships between molecular structure and charge transport are uncommon in the field of molecular electronics. Through a detailed mechanistic analysis of rectification and charge transport in BIPY-MCl_2 junctions, this work isolates the roles of molecular orbitals on the mechanisms of conductivity through molecular junctions. Furthermore, the mechanistic details described in this work are directly applicable to other molecular junctions, particularly those classified as having an insulating alkane chain terminated by a conductive moiety (i.e., conjugated aromatic group), and specifically how the frontier molecular orbitals influence the mechanism of conduction.

ASSOCIATED CONTENT

Supporting Information

The Supporting Information is available free of charge at https://pubs.acs.org/doi/10.1021/jacs.0c12641.

Nomenclature, details of experimental methods, statistical analysis, mechanism of tunneling, and general information (PDF)

AUTHOR INFORMATION

Corresponding Author

George M. Whitesides − *Department of Chemistry and Chemical Biology, Harvard University, Cambridge, Massachusetts 02138, United States;* orcid.org/0000-0001-9451-2442; Email: gwhitesides@gmwgroup.harvard.edu

Authors

Junwoo Park − *Department of Chemistry and Chemical Biology, Harvard University, Cambridge, Massachusetts 02138, United States*

Lee Belding − *Department of Chemistry and Chemical Biology, Harvard University, Cambridge, Massachusetts 02138, United States*

Li Yuan − *Department of Chemistry and Chemical Biology, Harvard University, Cambridge, Massachusetts 02138, United States*

https://dx.doi.org/10.1021/jacs.0c12641
J. Am. Chem. Soc. 2021, 143, 2156−2163

Maral P. S. Mousavi − *Department of Chemistry and Chemical Biology, Harvard University, Cambridge, Massachusetts 02138, United States*
Samuel E. Root − *Department of Chemistry and Chemical Biology, Harvard University, Cambridge, Massachusetts 02138, United States*
Hyo Jae Yoon − *Department of Chemistry and Chemical Biology, Harvard University, Cambridge, Massachusetts 02138, United States; Department of Chemistry, Korea University, Seoul 02841, Korea;* orcid.org/0000-0002-2501-0251

Complete contact information is available at: https://pubs.acs.org/10.1021/jacs.0c12641

Notes

The authors declare no competing financial interest.

■ ACKNOWLEDGMENTS

This work was supported by the National Science Foundation (NSF, CHE-18083681). We acknowledge the Materials Research and Engineering Center (MRSEC, DMR-1420570) at Harvard University for supporting XPS and UPS measurements, and providing access to the clean-room facilities. Sample characterization was performed in part at the Center for Nanoscale Systems (CNS) at Harvard University, a member of the National Nanotechnology Infrastructure Network (NNIN), which is supported by the National Science Foundation (ECS-0335765). J.P. acknowledges fellowship support from the Basic Science Research Program through the National Research Foundation of Korea (NRF), funded by the Ministry of Education of Korea (2018R1A6A3A03013079). HJY acknowledges the support from the NRF of Korea (NRF-2019R1-A2C2011003, NRF-2019R1A6A1A11044070) and the Future Research Grant (FRG) of Korea University. We thank Christian A. Nijhuis (Department of Chemistry, National University of Singapore), Victoria E. Campbell, and Philipp Rothemund for useful discussion and input. J.P. and G.M.W. conceived the research and designed the experiments. J.P., L.B., L.Y., M.P.S.M., S.E.R. and H.J.Y. performed the experiments and analyzed the data. L.B. performed the computational simulations. J.P., L.B., S.E.R., and G.M.W. wrote the manuscript.

■ REFERENCES

(1) Aviram, A.; Ratner, M. A. Molecular Rectifiers. *Chem. Phys. Lett.* **1974**, *29*, 277−283.
(2) Martin, A. S.; Sambles, J. R.; Ashwell, G. J. Molecular Rectifier. *Phys. Rev. Lett.* **1993**, *70*, 218−221.
(3) Capozzi, B.; Xia, J.; Adak, O.; Dell, E. J.; Liu, Z. F.; Taylor, J. C.; Neaton, J. B.; Campos, L. M.; Venkataraman, L. Single-Molecule Diodes with High Rectification Ratios through Environmental Control. *Nat. Nanotechnol.* **2015**, *10*, 522−527.
(4) Chen, X.; Roemer, M.; Yuan, L.; Du, W.; Thompson, D.; Del Barco, E.; Nijhuis, C. A. Molecular Diodes with Rectification Ratios Exceeding 10^5 Driven by Electrostatic Interactions. *Nat. Nanotechnol.* **2017**, *12*, 797−803.
(5) Carroll, R. L.; Gorman, C. B. The Genesis of Molecular Electronics. *Angew. Chem., Int. Ed.* **2002**, *41*, 4378−4400.
(6) Metzger, R. M. Unimolecular Electrical Rectifiers. *Chem. Rev.* **2003**, *103*, 3803−3834.
(7) Wold, D. J.; Frisbie, C. D. Fabrication and Characterization of Metal-Molecule-Metal Junctions by Conducting Probe Atomic Force Microscopy. *J. Am. Chem. Soc.* **2001**, *123*, 5549−5556.
(8) Song, H.; Reed, M. A.; Lee, T. Single Molecule Electronic Devices. *Adv. Mater.* **2011**, *23*, 1583−1608.
(9) Chabinyc, M. L.; Chen, X.; Holmlin, R. E.; Jacobs, H.; Skulason, H.; Frisbie, C. D.; Mujica, V.; Ratner, M. A.; Rampi, M. A.; Whitesides, G. M. Molecular Rectification in a Metal-Insulator-Metal Junction Based on Self-Assembled Monolayers. *J. Am. Chem. Soc.* **2002**, *124*, 11730−11736.
(10) Kornilovitch, P. E.; Bratkovsky, A. M.; Stanley Williams, R. Current Rectification by Molecules with Asymmetric Tunneling Barriers. *Phys. Rev. B: Condens. Matter Mater. Phys.* **2002**, *66*, 1−11.
(11) Liu, R.; Ke, S. H.; Yang, W.; Baranger, H. U. Organometallic Molecular Rectification. *J. Chem. Phys.* **2006**, *124*, 244705.
(12) Nijhuis, C. A.; Reus, W. F.; Whitesides, G. M. Molecular Rectification in Metal-SAM-Metal Oxide-Metal Junctions. *J. Am. Chem. Soc.* **2009**, *131*, 17814−17827.
(13) Nitzan, A. Electron Transmission through Molecules and Molecular Interfaces. *Annu. Rev. Phys. Chem.* **2001**, *52*, 681−750.
(14) Tao, N. J. Electron Transport in Molecular Junctions. *Nat. Nanotechnol.* **2006**, *1*, 173−181.
(15) Nichols, R. J.; Higgins, S. J. Single-Molecule Electronics: Chemical and Analytical Perspectives. *Annu. Rev. Anal. Chem.* **2015**, *8*, 389−417.
(16) Marcus, R. A. Electron Transfer Reactions in Chemistry. Theory and Experiment. *Rev. Mod. Phys.* **1993**, *65*, 599−610.
(17) Liang, W.; Shores, M. P.; Bockrath, M.; Long, J. R.; Park, H. Kondo Resonance in a Single-Molecule Transistor. *Nature* **2002**, *417*, 725−729.
(18) Venkataraman, L.; Klare, J. E.; Nuckolls, C.; Hybertsen, M. S.; Steigerwald, M. L. Dependence of Single-Molecule Junction Conductance on Molecular Conformation. *Nature* **2006**, *442*, 904−907.
(19) Lindsay, S. M.; Ratner, M. A. Molecular Transport Junctions: Clearing Mists. *Adv. Mater.* **2007**, *19*, 23−31.
(20) Song, H.; Kim, Y.; Jang, Y. H.; Jeong, H.; Reed, M. A.; Lee, T. Observation of Molecular Orbital Gating. *Nature* **2009**, *462*, 1039−1043.
(21) Coropceanu, V.; Chen, X.-K.; Wang, T.; Zheng, Z.; Brédas, J.-L. Charge-Transfer Electronic States in Organic Solar Cells. *Nat. Rev. Mater.* **2019**, *4*, 689−707.
(22) Yoon, H. J.; Liao, K. C.; Lockett, M. R.; Kwok, S. W.; Baghbanzadeh, M.; Whitesides, G. M. Rectification in Tunneling Junctions: 2,2'-Bipyridyl-Terminated n-Alkanethiolates. *J. Am. Chem. Soc.* **2014**, *136*, 17155−17162.
(23) Kang, H.; Kong, G. D.; Byeon, S. E.; Yang, S.; Kim, J. W.; Yoon, H. J. Interplay of Fermi Level Pinning, Marcus Inverted Transport, and Orbital Gating in Molecular Tunneling Junctions. *J. Phys. Chem. Lett.* **2020**, *11*, 8597−8603.
(24) Powell, C. J.; Jablonski, A. Electron Effective Attenuation Lengths for Applications in Auger Electron Spectroscopy and X-Ray Photoelectron Spectroscopy. *Surf. Interface Anal.* **2002**, *33*, 211−229.
(25) Vericat, C.; Vela, M. E.; Benitez, G.; Carro, P.; Salvarezza, R. C. Self-Assembled Monolayers of Thiols and Dithiols on Gold: New Challenges for a Well-Known System. *Chem. Soc. Rev.* **2010**, *39*, 1805−1834.
(26) Constable, E. C.; Housecroft, C. E. The Early Years of 2,2'-Bipyridine—A Ligand in Its Own Lifetime. *Molecules* **2019**, *24*, 3951.
(27) Murali, M.; Palaniandavar, M. Mixed-Ligand Copper(II) Complexes with Positive Redox Potentials. *Transition Met. Chem.* **1996**, *21*, 142−148.
(28) Upadhyay, D. N.; Yegnaraman, V.; Rao, G. P. Hexacyanoferrate Modification of Gold Electrode through Monolayer Approach. *Langmuir* **1996**, *12*, 4249−4252.
(29) Freire, R. S.; Kubota, L. T. Electrochemical Behavior of the Bis(2,2'-Bipyridyl)Copper(II) Complex Immobilized on a Self-Assembled Monolayer Modified Electrode for L-Ascorbic Acid Detection. *Analyst* **2002**, *127*, 1502−1506.
(30) Allen, J. B.; Larry, R. F. *Electrochemical Methods Fundamentals and Applications*; John Wiley & Sons: 2001.
(31) Byeon, S. E.; Kim, M.; Yoon, H. J. Maskless Arbitrary Writing of Molecular Tunnel Junctions. *ACS Appl. Mater. Interfaces* **2017**, *9*, 40556−40563.

(32) Beebe, J. M.; Kim, B.; Gadzuk, J. W.; Frisbie, C. D.; Kushmerick, J. G. Transition from Direct Tunneling to Field Emission in Metal-Molecule-Metal Junctions. *Phys. Rev. Lett.* **2006**, *97*, 1−4.

https://dx.doi.org/10.1021/jacs.0c12641
J. Am. Chem. Soc. 2021, 143, 2156−2163